




Cite this: DOI: 10.1039/c9ob01132c

Design, screening and biological evaluation of novel fatty acid chain-modified oxyntomodulin-based derivatives with prolonged glucose-lowering ability and potent anti-obesity effects†

Lei Zhao,^a Baohua Wang,^a Limin Wang,^a Xie Zhao,^b Zhe Chen^c and Lixia Sun  ^{*a}

Recently, oxyntomodulin (OXM) has emerged as a treatment option for type 2 diabetes mellitus and obesity. In order to develop more promising novel OXM derivatives combining glycemic effects of glucagon-like peptide-1 (GLP-1) and lipolytic properties of glucagon, six 12-mer GLP-1 receptor agonists (PP01–PP06) were screened using a phage display method and then fused to OXM (3–37) to generate hybrid OXM derivatives (PP07–PP12). PP11, as a selected starting point, was further site-specifically modified with three lengths of fatty acid chains to provide long-acting conjugates PP13–PP24, among which PP18 was found not only to retain almost the entire balanced activation potency of PP11 in GLP-1/glucagon receptors but also to enhance plasma stability and prolong hypoglycemic activity. PP18 was further confirmed as an insulin secretagogue and glycemic agent in gene knockout mice. The protracted antidiabetic effects and *in vivo* half-life of PP18 were further proved by hypoglycemic efficacies in diet-induced obesity (DIO) mice and pharmacokinetics tests in Sprague Dawley (SD) rats, respectively. Nevertheless, administration of PP18 once per day normalized food intake, body weight, blood biochemical indexes, insulin resistance and islet function of DIO mice. These preclinical results suggested that PP18, as a novel OXM-based dual GLP-1 and glucagon receptor agonist, may serve as a novel therapeutic approach to treat T2DM and obesity.

Received 15th May 2019,
Accepted 17th July 2019

DOI: 10.1039/c9ob01132c

rsc.li/obc

Introduction

Type 2 diabetes mellitus (T2DM) is a complex metabolic disorder characterized by hyperglycemia arising from a combination of insufficient insulin secretion and the development of insulin resistance.^{1,2}

Oxyntomodulin (OXM) is a 37-amino acid peptide of the proglucagon-derived peptide family, and it is secreted postprandially by intestine L-cells.³ It shows high sequence homology to GLP-1 and glucagon. OXM decreases both food intake and body weight, and it increases the secretion of insulin and maintains glucostasis.^{4–7} The mechanisms of the potential hypoglycemic and anti-obesity effects of OXM were reported to have a dual-mode of action mediated through co-activation of both the glucagon receptor (GcgR) and the GLP-1 receptor

(GLP-1R), although it had weaker potency (1/10–1/100) compared to native GLP-1 and glucagon.⁸ Previous studies have hypothesized that OXM activates the function of the GLP-1 receptor to promote glycometabolism by stimulating the secretion of insulin and further co-activating GcgR, which enhances a reduction in food intake and body weight.^{9,10} The C-terminal regions of OXM interact with the N-terminal extracellular domain of GLP-1R. This facilitates the interaction with the transmembrane domain of the receptor, which leads to receptor activation.^{11,12} Therefore, OXM-based peptides have potential because a fruitful avenue for the search for relevant new agents remains a major medical need, especially for those that have dual effects on diabetes and obesity.

However, the clinical utility of OXM is critically limited due to its short *in vivo* half-life, which is due to its rapid degradation and clearance by dipeptidyl peptidase IV (DPP-IV) and renal excretion, respectively.¹³ After the removal of the N-terminal dipeptide using DPP-IV, the intact OXM is changed to OXM (3–37), which has no bioactivity and behaves as a competitive antagonist. The therapeutic utility of OXM is limited due to its short *in vivo* half-life and unbalanced activation potency in GLP-1 and glucagon receptors. Thus, OXM analogues with low renal clearance and high DPP-IV-resistance

^aNorth China University of Science and Technology Affiliated Hospital, Tangshan, Hebei 063000, P.R. China. E-mail: lxsun@ncstmc.cn; Tel: +86-315-3725120

^bPeking University, College of Pharmaceutical Sciences, Beijing, 100000, P.R. China

^cNorth China University of Science and Technology, Tangshan, Hebei 063000, P.R. China

†Electronic supplementary information (ESI) available. See DOI: 10.1039/c9ob01132c

that have prolonged *in vivo* activity should be considered to be a research direction for the development of OXM-based drugs.^{14,15}

By obtaining a better understanding of the potential physiological consequences of OXM due to pleiotropic signaling of both GLP-1R and GcgR, we can provide new avenues for the development of anti-diabetes and obesity drugs that have greater therapeutic value and less side effects. In this work, we aimed at designing candidates with enhanced effects on GLP-1 receptor activation and free of DPP-IV cutting sites leading to prolonged *in vivo* activity. Thus, we designed and constructed novel OXM-based hybrid peptides using phage display and peptide fusion. Further side-chain modification was conducted with selected PP11. However, appropriate modification sites and fatty chain lengths are directly related to the bioactivity of hybrid peptides. So we conducted structure–activity studies including dual GLP-1/glucagon receptor activation potency, plasma stability and *in vivo* hypoglycemic durability to avoid any bioactivity loss. The ultimately selected molecule was further carefully evaluated *in vivo*.

Results

The discovery of PP11 as a lead peptide with a balanced affinity for GLP-1R and GcgR

OXM is a natural dual agonist and induces both GLP-1R- and GcgR-mediated cAMP production, although it exhibits weaker potency (1/10–1/100) compared to native GLP-1. However, its short *in vivo* half-life and unbalanced activation potency in GLP-1 and glucagon receptors limit the use of OXM in clinical applications.

To preserve the natural structure–activity relationships and enhance anti-enzymatic hydrolysis ability of OXM, we chose to

screen and identify the newly designed OXM derivatives. Under the guidance of this object, we used a commercial peptide library, containing 12 linear random peptide sequences, to discover the GLP-1R-binding domain without the DPP-IV digestion site. As a result, the six peptides (termed PP01–PP06) were selected from peptide libraries with an affinity for GLP-1R extracellular domain (ECD) after four rounds of selection.

As shown in Fig. 1, the selected PP01–PP06 peptides were fused to the N-terminus of OXM 3–37 using a short linker (GG), and six hybrid peptides (termed PP07–PP12), with not only higher potency in GLP-1R but also better resistance to DPP-IV, were generated and further detected using high-performance liquid chromatography (HPLC) and mass spectrum (MS) analysis (ESI, Fig. S1 and Tables S1, S2†). Surface plasmon resonance (SPR) measurements showed that PP11 had a more balanced binding affinity for GLP-1R and GcgR, with a K_d value of 0.66 and 1.15 μM , respectively (Table 1), compared to the other peptides.

Synthesis and screening of fatty chain-modified OXM-based dual receptor agonists

Therefore, we chose PP11 as the principal sequence for further side-chain modifications to extend its predicted short *in vivo* half-life. As shown in Fig. 2, lysine scanning mutagenesis was performed to determine a suitable acylation site. The original lysines (24 and 42) and selected lysine altered (Q15K and A49K) sequences were reacted with different lengths of gamma-glutamates (C12, C16, and C18), which were selected from semaglutide,¹⁶ to extend the plasma half-life by facilitating reversible binding to albumin.^{17–19} Twelve modified products (PP13–PP24) were synthesized and characterized using HPLC and MS (ESI, Fig. S1 and Tables S1, S2†). The obtained peptides were further evaluated by human GLP-1 and glucagon receptor activation experiments. As shown in Table 2, we found that the GLP-1 receptor activation potency was closely related to the sites of side-chain modifications. The N-terminal- (PP13–PP15) or C-terminal-modified analogues (PP19–PP21 and PP22–PP24) showed weaker potency compared to that of middle-modified analogues (PP16–PP18), suggesting that lysine-specific conjugations to the N- or C-terminal affect the binding and activating function of the selected 12-mer GLP-1R agonist or OXM (31–37), a reported GLP-1R binding sequence. Furthermore, we found that the dual receptor activation potency was hardly independent of

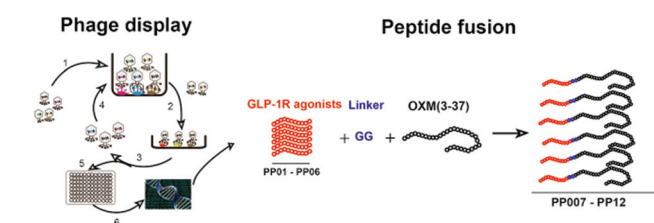


Fig. 1 Schematic diagram of the discovery of novel OXM-based analogues.

Table 1 Binding affinity of selected peptides and OXM analogues for GLP-1R and GcgR ECD

Peptide	Sequence	GLP-1R K_d (μM)	Peptide	Sequence	GLP-1R K_d (μM)	GcgR K_d (μM)
PP01	AACVCFTCVLV	1.25	PP07	AACVCFTCVLV-GG-OXM(3-37)	3.95	1.224
PP02	ACSHSGFCVLAG	2.12	PP08	ACSHSGFCVLAG-GG-OXM(3-37)	1.88	1.151
PP03	AGVMIDQRLACA	1.55	PP09	AVMIDQRLACAA-GG-OXM(3-37)	1.42	1.253
PP04	GACALEVDCAGA	1.56	PP10	GACALEVDCAGA-GG-OXM(3-37)	4.31	3.998
PP05	ACAELVDNAVAI	0.51	PP11	ACAELVDNAVAI-GG-OXM(3-37)	0.66	1.152
PP06	HGVCPCQVCVI	1.79	PP12	HGVCPCQVCVI-GG-OXM(3-37)	2.99	1.092

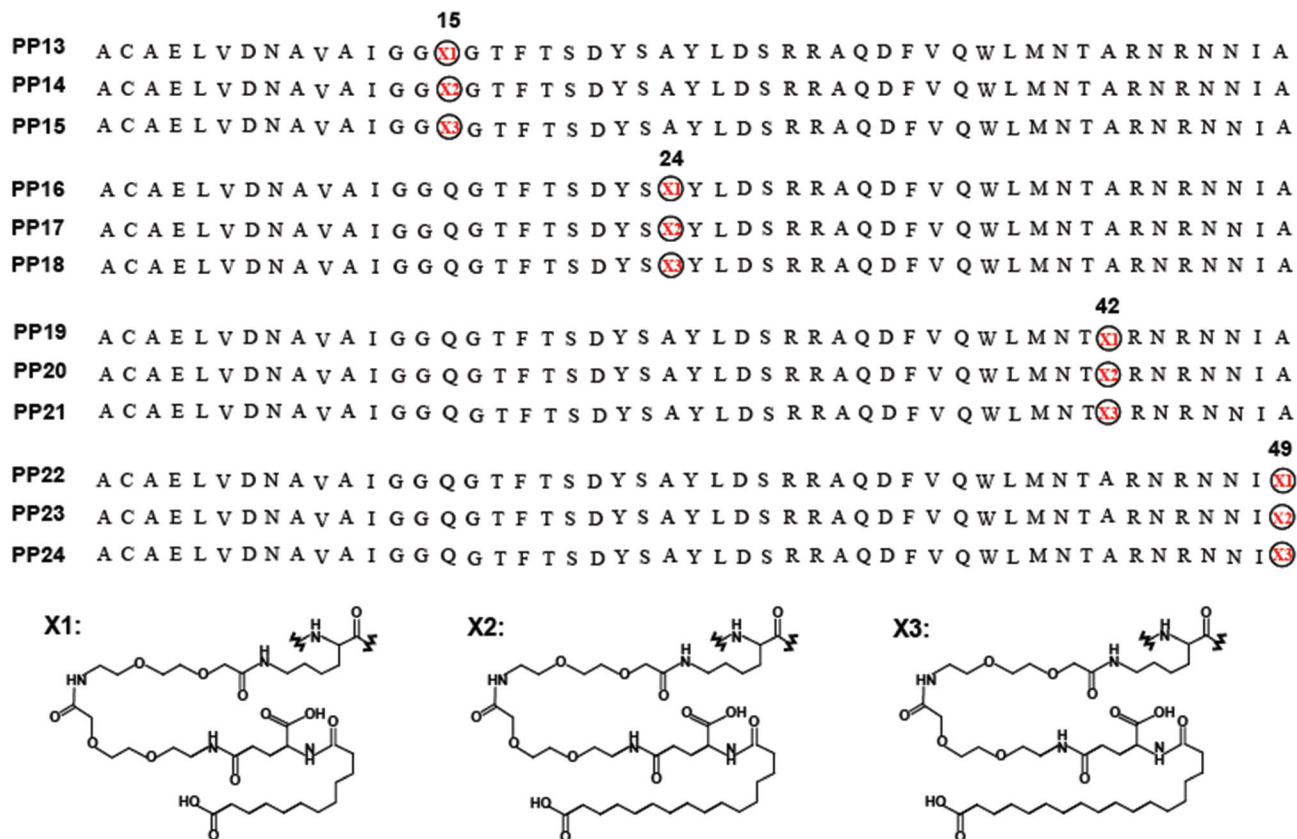


Fig. 2 Structures of twelve fatty chain-modified OXM-based conjugates.

Table 2 *In vitro* pharmacological characterization of fatty chain-modified OXM analogues for stably expressed GLP-1R and GcgR

Peptide	Human GLP-1R		Human GcgR	
	EC ₅₀ (nM)	Relative (%)	EC ₅₀ (nM)	Relative (%)
GLP-1	0.451	89	>100	<1
Glucagon	1.352	32	0.152	100
OXM	0.691	76	0.185	92
PP11	0.352	100	0.178	94
PP13	0.411	94	0.195	91
PP18	0.487	88	0.188	93
PP15	0.427	92	0.202	83
PP16	1.598	28	0.231	78
PP17	1.418	41	0.156	96
PP18	1.312	35	0.189	93
PP19	0.887	63	0.261	70
PP20	0.795	71	0.212	78
PP21	0.777	70	0.246	74
PP22	1.215	44	0.171	95
PP23	1.012	56	0.185	92
PP24	1.011	56	0.157	98

the fatty chain length as the analogues (PP16–PP18) showed similar receptor activation potency (Table 2). We further evaluated the *in vitro* plasma stability of OXM-based analogues (PP16–PP18). Shown in Fig. 3 is the percentage–time curve of the intact peptide of OXM, PP11, and its side-chain modified analogues after incubation with rat plasma for 72 h at 37 °C.

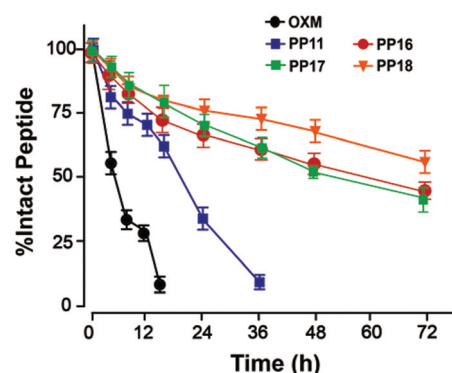


Fig. 3 *In vitro* plasma stability test. All data are expressed as mean \pm SD ($n = 5$).

Native OXM was rapidly degraded and has an estimated half-life of 3.1 h. The 72 h residual percentage of side-chain modified analogues (PP16–PP18) was closely related to the length of the fatty chain as analogues with longer fatty chains showed better stability than those with shorter fatty chains. The residual percentage of PP18 remained above 60% at 72 h using the original concentration of 100%.

We further evaluated the hypoglycemic durabilities of the selected PP16–PP18 in DIO mice using a modified multiple

method. Overnight fasting DIO mice were administered with 2 g kg^{-1} glucose half an hour after intraperitoneal injection of saline, liraglutide, (30 nmol kg^{-1}) and PP16–PP18 (30 nmol kg^{-1}). As shown in Fig. 4, BGLs in saline-treated mice rapidly increased over 27 mmol L^{-1} within 0.5 hours, while those of liraglutide or OXM-based analogues were less than 20 mmol L^{-1} . After the second administration of glucose at 24 h, liraglutide was almost ineffective and a similar result was shown in the PP16-treated group after the third glucose administration. In contrast, PP18 exhibits long-lasting hypoglycemic effects during the whole testing period (0–50 h). The above results demonstrated that PP18 was a better glucose-lowering agent compared to PP16–PP17.

The binding affinity of PP18 for GLP-1R and GcgR was also evaluated using SPR measurements (ESI, Fig. S2†). Since PP18 exhibits not only balanced dual receptor activation potency which was similar to that of native GLP-1 or glucagon, respectively, but also better *in vitro* plasma stability or *in vivo* hypo-

glycemic durability, we selected this molecule for further efficacy evaluation.

In vitro pharmacological characterization of PP11 and PP18

PP11 and PP18 were designed to be potent for both GLP-1R and GcgR to allow significant target engagement of both receptors. We further utilized Chinese hamster ovary (CHO) cells stably expressing GLP-1R, GcgR, or both to assess signaling in cells expressing endogenous levels of these receptors. PP11- and PP18-induced cAMP production was significantly higher than that of the vehicle, and it was similar to that of native GLP-1 or glucagon in GLP-1 or glucagon receptor activation, respectively (Fig. 5A and B). As shown in Fig. 5C, native GLP-1 and glucagon activate their respective receptors, and they resulted in similar levels of cAMP. However, both PP11 and PP18 elicited a significantly higher cAMP response than either GLP-1 or glucagon, and they were similar to the co-incubation of GLP-1 and glucagon. In addition, cAMP pro-

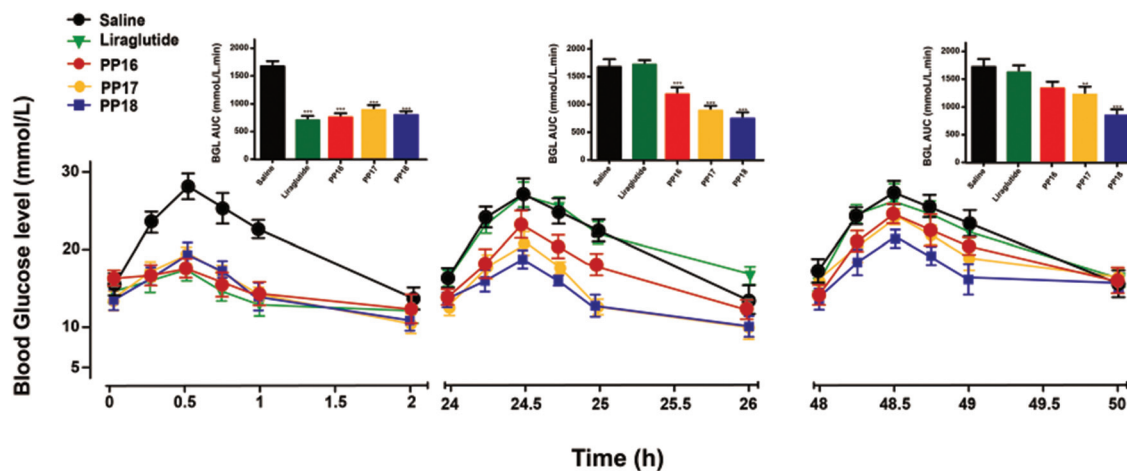


Fig. 4 Long-time glucose-lowering effect of OXM-based analogues were studied using multiple IPGTTs in DIO mice. $P < 0.05$, 0.02 , and 0.001 using one-way ANOVA versus control group (*, **, and ***). All data are expressed as mean \pm SD ($n = 6$).

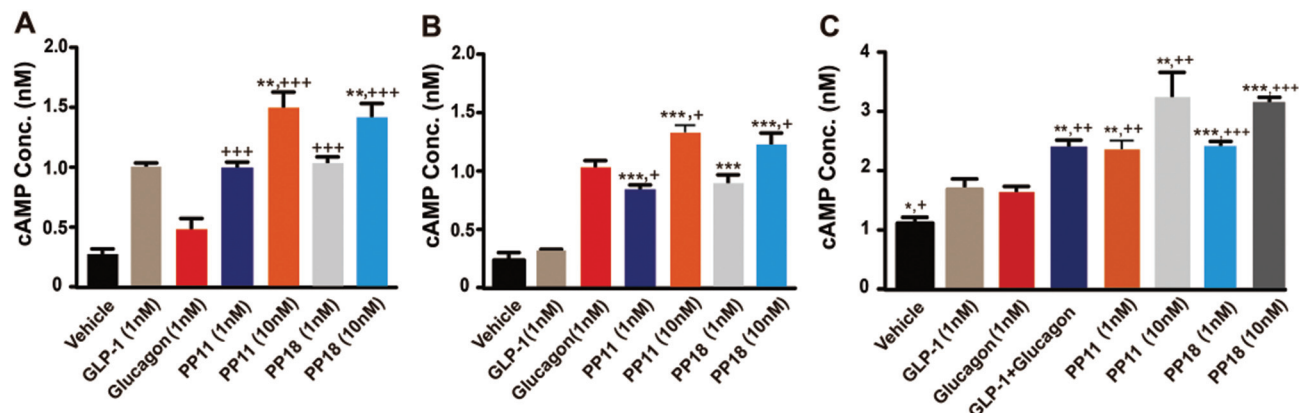


Fig. 5 cAMP accumulation in CHO cells expressing (A) GLP-1R, (B) GcgR or (C) both. $P < 0.05$, 0.02 , and 0.001 using one-way ANOVA versus GLP-1 (*, **, and ***) or GIP (+, ++, and +++). All data are expressed as mean \pm SD ($n = 3$).

duction was induced by PP11 and PP18 in a dose-dependent manner.

Acute administration of PP18 stimulates insulin secretion and lowers glucose in knockout mice

We utilized wild-type (WT) mice that express both GLP-1 and glucagon receptor and transgenic mice that lack GLP-1R (GLP-1R^{-/-}) or GcgR (GcgR^{-/-}) to examine the effects of OXM-based analogues on insulin secretion. As shown in Fig. 6A, insulin secretion in islets from WT mice was stimulated by PP11 and PP18 in a glucose-dependent manner. However, in the GLP-1R knockout mice, the insulin secretion of PP11 and PP18 were almost completely blocked, as predicted (Fig. 6B).

Similar results were observed in GcgR^{-/-} mice following incubation with the GLP-1R antagonist (Fig. 6C). This demonstrates the specificity of PP11 and PP18 for GLP-1R in insulin secretion.

We further evaluated the glycemic control effects of PP18 using IPGTT in the above-mentioned mice. PP18 improved the glucose tolerance in WT mice (Fig. 6D) in a dose-dependent manner, and the response was comparable to that observed for liraglutide. Furthermore, GLP-1R deficiency abolished the reduction in glucose caused by PP18 or liraglutide (Fig. 6E). Interestingly, the activation of the glucagon receptor by PP18 did not induce a significant elevation in blood glucose (Fig. 6F). Together, these results indicate that PP18 can induce

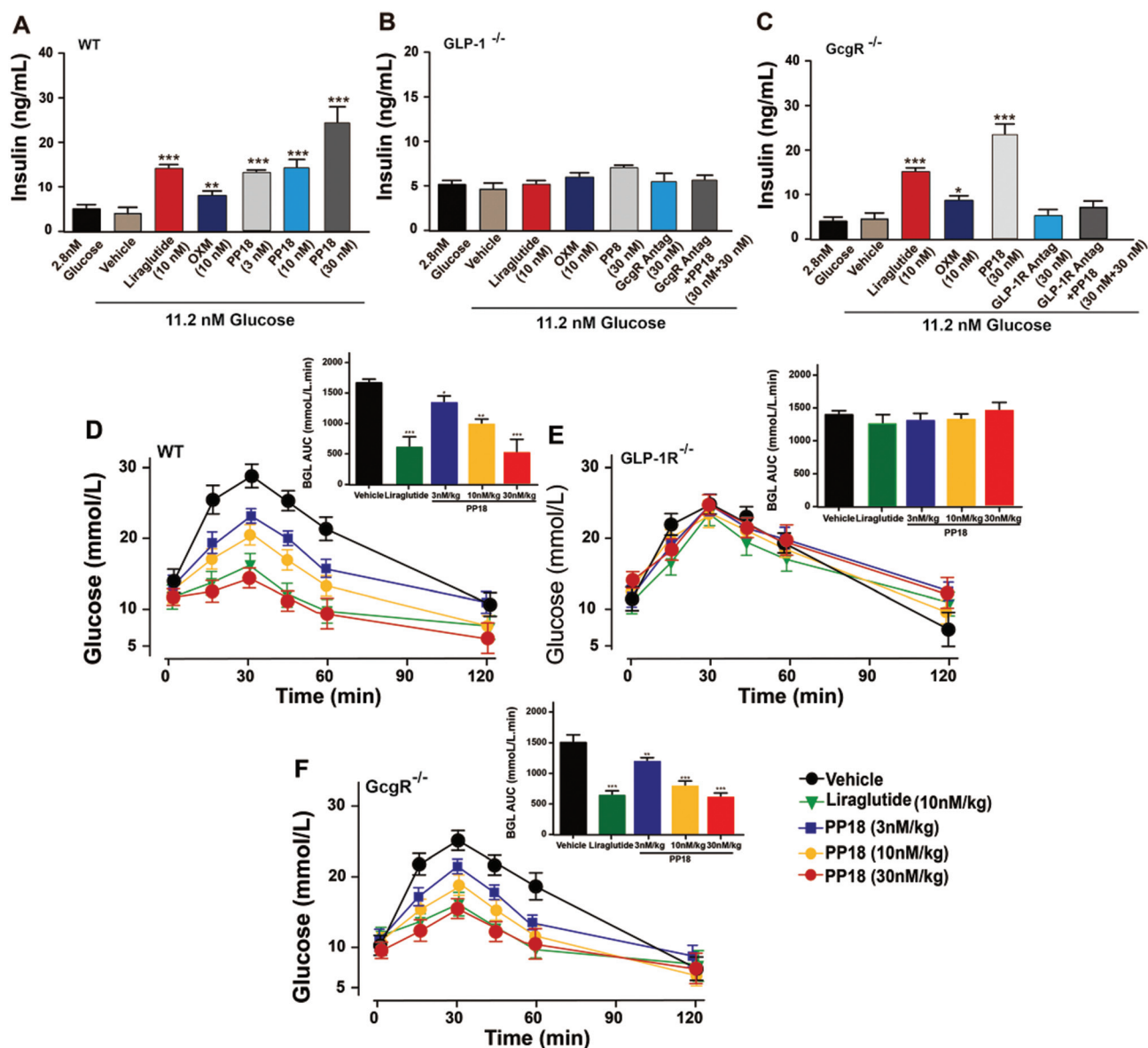


Fig. 6 Insulin secretion and glucoregulatory assays. OXM analogues enhance insulin secretion of the islet from wild-type (A), GLP-1 receptor null (B), and glucagon receptor null (C) mice ($n = 3$). PP18 improves glucose tolerance in wild-type (A), GLP-1 receptor null (B), and glucagon receptor null (C) mice. * $P < 0.05$, ** $P < 0.02$, and *** $P < 0.001$ using one-way ANOVA versus vehicle. All data are expressed as mean \pm SD ($n = 6$).

glucose-dependent insulin secretion *in vitro* and *in vivo* through GLP-1R, and the activation of glucagon did not cause an obvious elevation in blood glucose.

Hypoglycemic duration tests

The hypoglycemic duration of PP18 was carefully evaluated for two doses (10 or 30 nmol kg⁻¹, s.c. injection) in DIO mice. A blood glucose level below 8.35 mmol L⁻¹ was regarded as normal, and euglycemic duration below this value is considered as the potential to become anti-diabetic therapeutics. As shown in Fig. 7, BGLs in PBS-treated mice still higher maintained a hyperglycemic state (average >20 mmol L⁻¹), whereas administration of liraglutide (30 nmol kg⁻¹) or PP18 (10 or 30 nmol kg⁻¹) rapidly lowered the blood glucose to normal levels within 3 h after a subcutaneous single-dose injection. Notably, PP18 showed much longer hypoglycemic durations compared to native liraglutide for both doses (10 or 30 nmol kg⁻¹). The time of two doses of PP18-treated rats required to rebound to a glucose level of 8.35 mmol L⁻¹ was ~25 h (10 nmol kg⁻¹) and ~36 h (30 nmol kg⁻¹) as compared with 4 h for liraglutide (10 nmol kg⁻¹) treated rats. Furthermore,

PP18 showed glucose-lowering percentages of 23.5% and 58.3% at a low or high dose for 0–96 h compared with PBS, respectively (Fig. 7B).

Pharmacokinetics tests

As illustrated in Fig. 7C, the pharmacokinetic properties of PP18 were further evaluated in SD rats which were administered a single right forelimb intravenous injection of 30 nmol kg⁻¹ PP18. After the injection, the plasma concentration of OXM rapidly declined to a baseline at 6 h post-injection, and it had a calculated elimination half-life ($t_{1/2}$) of 2.1 ± 0.6 h. As expected, the elimination half-life ($t_{1/2}$ = 38.5 ± 5.9 h) of PP18 was significantly extended by the modification of the fatty acid chain.

Chronic administration of PP18 in DIO mice

To determine whether chronic treatment with the OXM-based dual-receptor agonist can improve hyperglycemia and obesity, DIO mice were treated daily with liraglutide (10 nM kg⁻¹) or PP18 (10, 30 nM kg⁻¹) for 4 weeks. Both liraglutide and PP18 significantly decreased food intake and body weight (Fig. 8A–C) during treatment, compared to vehicle-treated

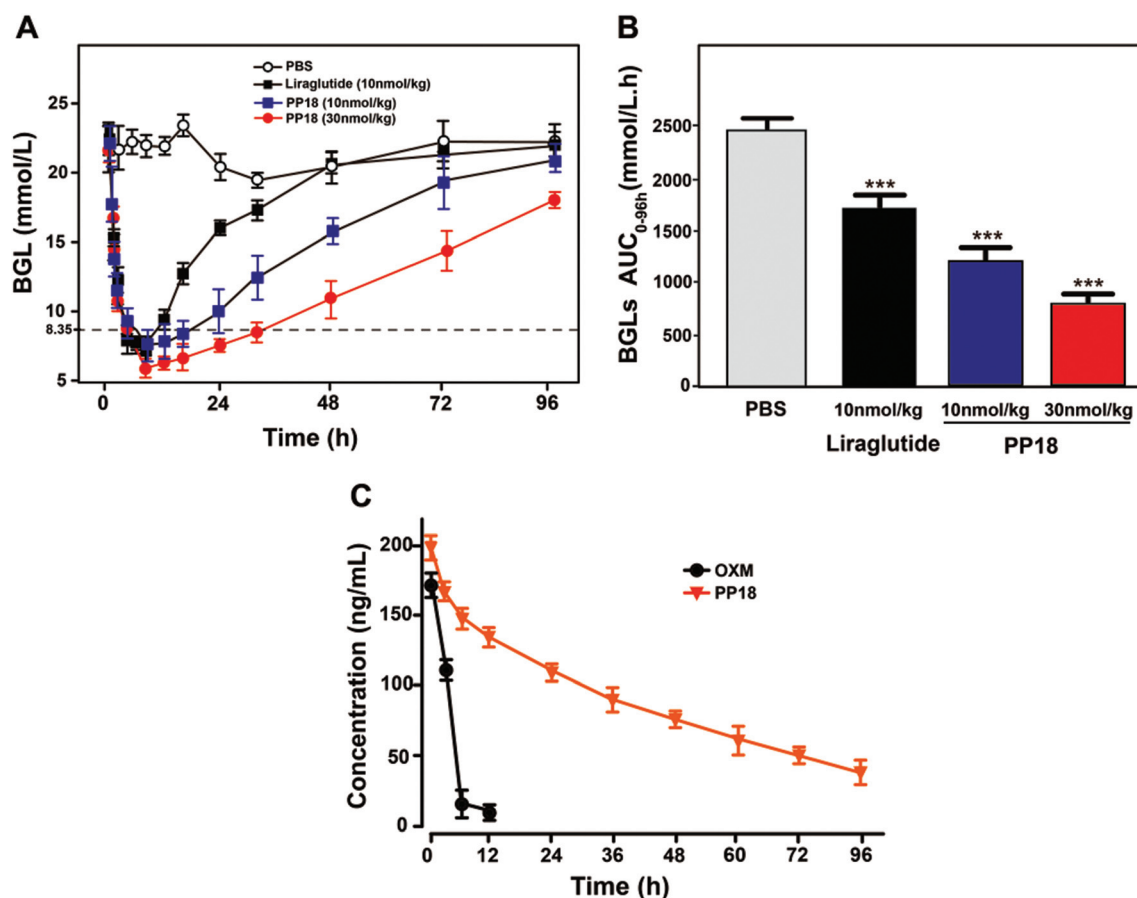


Fig. 7 Glucose-stabilizing effect and pharmacokinetics test of PP18. (A) Time-course average blood glucose levels of db/db mice after a single dose of PBS, liraglutide (10 nmol kg⁻¹), PP18 (10 or 30 nmol kg⁻¹). (B) Hypoglycemic effects based on AUC_{0-96h}. Results are presented as mean ± SD (n = 8 each group). *** P < 0.001, ** P < 0.02, and * P < 0.05. (C) Pharmacokinetic profile of PP18 in SD rats. Results are presented as mean ± SD (n = 6 each group).

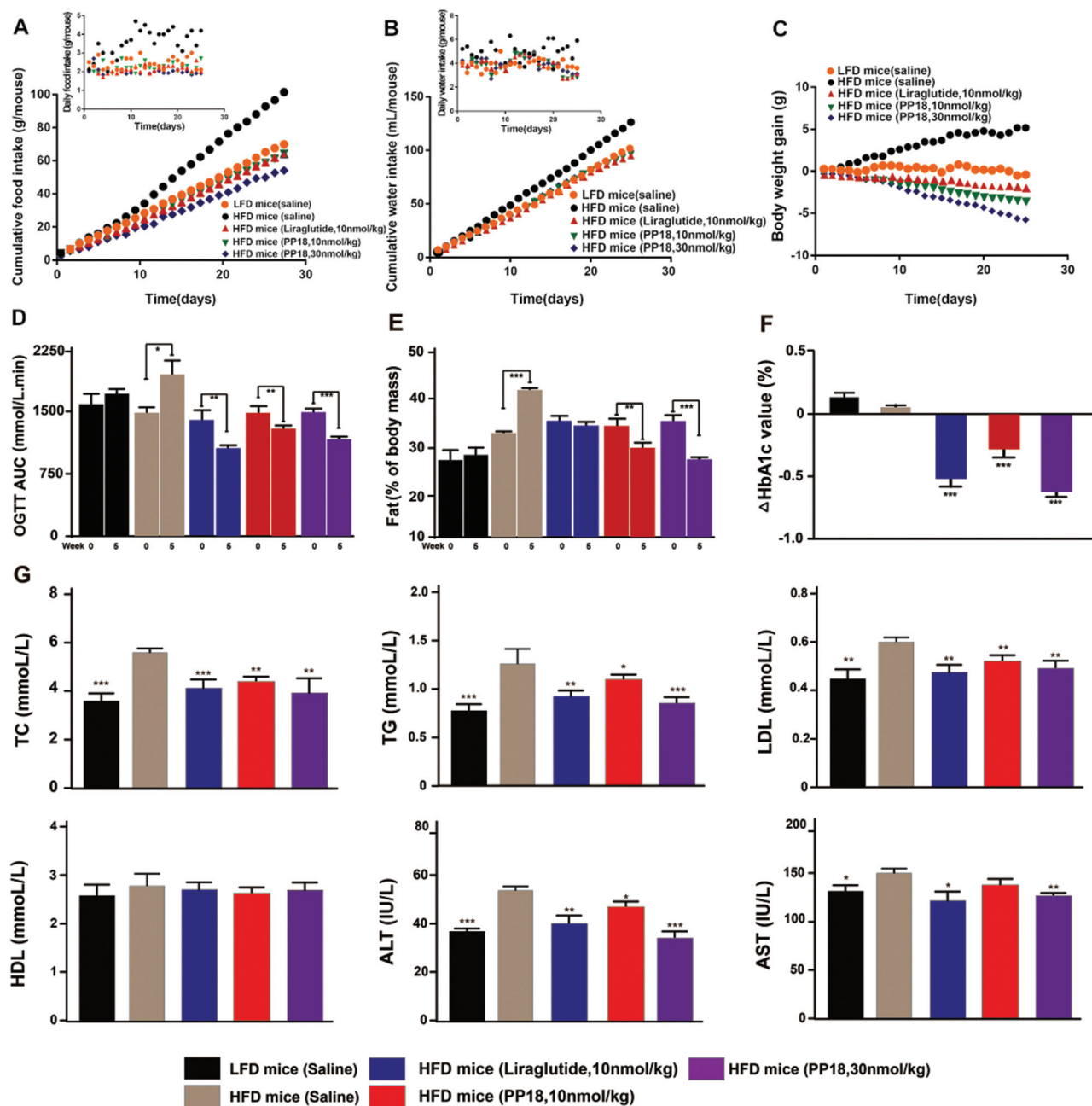


Fig. 8 Chronic administration of PP18 improves glycemia and obesity in DIO mice. Effect on food intake (A), water intake (B), body weight gain (C), glucose tolerance (D), fat mass (E), HbA1c levels (F), and blood biochemistry indexes (G) following daily subcutaneous injection of saline, liraglutide, or PP18 at 30 nmol kg⁻¹ in db/db mice. Results are presented as mean \pm SD. * P < 0.05, ** P < 0.02, and *** P < 0.001 versus vehicle in HFD mice, and n = 8 each group.

high-fat feeding (HFD) mice or low-fat feeding (LFD) mice. Additionally, PP18 showed better control of food intake and body weight compared to liraglutide at both the same (10 nmol kg⁻¹) or higher dose (30 nmol kg⁻¹).

We next determined whether a similar improvement in insulin-resistance can be observed in DIO mice. In the first week, DIO mice were overnight fasted (~15 h), and then an IPGTT was conducted to determine the blood glucose pre-dose and at 15, 30, 60, 90, and 120 min after glucose adminis-

tration. As shown in Fig. 8D, the blood glucose levels and areas under the curve (AUC) for the liraglutide- and PP18-treated groups were not significantly different compared to the control group (P > 0.05, n = 8). However, after 4 weeks, an IPGTT revealed that the AUC of the PP18 group was decreased by almost 25% compared to the results determined in the same mice at week 0. An IPGTT without an injection of PP18 was conducted after a week of wash-out. Unsurprisingly, there was a significant reduction in glucose (P < 0.001, n = 8)

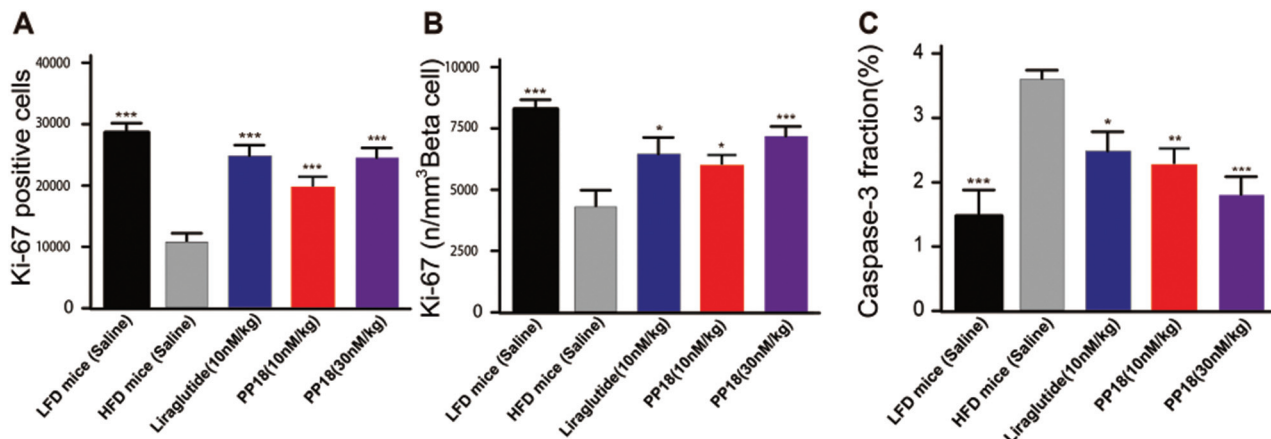


Fig. 9 Effects of 4 weeks of treatment with PP18 on the stereological estimation of the total number (A) and the density (B) of Ki-67-positive beta cells, and the caspase-3 fraction (caspase-3 mass in percent of the islet mass) (C). Results are presented as mean \pm SD. * P < 0.05, ** P < 0.02, and *** P < 0.001 versus vehicle, and n = 8 each group.

observed in PP18-treated mice compared to control mice, and it was similar to the liraglutide-treated mice.

Then, we measured the HbA1c levels as an index of long-term blood glucose regulation in DIO mice treated with PP18 for 4 weeks. Two doses of PP18 were tested, and in both doses, a significant decrease in HbA1c was observed compared to the control. However, the decrease was less in liraglutide-treated mice (Fig. 8F). The superior effect of PP18 in lowering HbA1c levels correlates well with its superior efficacy in lowering both fasting and non-fasting blood glucose levels. Chronic treatment with PP18 resulted in a significant dose-dependent decrease in body weight (Fig. 8C). This response was more pronounced than the response observed with the two doses of PP18, and it was primarily driven by the loss of fat mass (Fig. 8E). However, an equivalent dose of liraglutide had no effect. It appears that PP18 mainly produced a larger and more prolonged reduction in fat consumption.

Chronic treatment with PP18 at both doses significantly reduced triglycerides, total cholesterol, and low-density lipoprotein levels without affecting high-density lipoprotein, when compared to the administration of a saline control (Fig. 8G). Importantly, chronic treatment with PP18 did not induce hepatocellular toxicity, as reflected by the absence of changes in plasma levels of alanine aminotransferase and aspartate aminotransferase (Fig. 8G).

Treatment with PP18 for 4 weeks significantly increased both the total number and density of proliferating Ki-67-immunoreactive beta cells (Fig. 9A and B, Fig. S3A†) compared to the vehicle control (P < 0.001). In contrast, a trend toward a reduction in the caspase-3 percentage (the caspase-3 mass in percent of the islet mass) was observed in both doses of PP18-treated groups (Fig. 9C and Fig. S3B†).

Collectively, these data suggest that chronic treatment with a dual GLP-1 and glucagon receptor agonist reduces body weight by reducing food intake and increasing fat consumption, and it could improve the symptoms of insulin resistance

and abnormal blood biochemical indexes induced by a high-fat diet.

Discussion

Many diseases, especially the complex metabolic disease of T2DM, cannot be sufficiently treated with a single drug regimen. Recently, the development of a single entity that has combined, multiple, beneficial effects on metabolic hormones has become a new trend.^{20–23} Thus, ‘hybrid’ or ‘multiple-targeting’ peptides are actively being developed and evaluated for their properties as multi-action agents for weight loss and diabetes.²⁴

OXM is a natural dual agonist that induces both GLP-1R and GcgR-mediated cAMP production. Despite the 10–100 fold reduction in potency in the activation of GLP-1R, compared with the native GLP-1 ligand, OXM causes modest but stable anti-diabetic and anti-obesity effects, such as effects on weight loss, insulin secretion, and glucose homeostasis.²⁵ OXM is easily degraded by DPP-IV at position-2 (a naturally-occurring Ser) to produce OXM 3–37 (OXM lacking the 2 first amino acids), which limits its clinical utility. Thus, these liabilities of weak activation of GLP-1R, fast DPP-IV cleavage, and renal excretion should be addressed to improve its clinical applications.

In the present study, our newly designed peptides comprise a selected 12-mer GLP-1R agonist, a short linker and OXM (3–37). The N-terminal regions of OXM, a 37 amino acid peptide agonist interacts with the N-terminal extracellular domain of GLP-1R and GcgR, facilitating the interaction with the transmembrane domain of the receptor leading to receptor activation. The selected 12-mer GLP-1R agonists were screened using a phage display method and fused to OXM (3–37) to generate the OXM-based hybrid peptide. On the one hand, the DPP-IV cutting site of OXM was replaced by fusing the selected

12-mer peptide to N-terminal of OXM (3–37). On the other hand, these peptides were developed by combining the glycaemic and anorectic effects of GLP-1 with the lipolytic and thermogenic properties of glucagon. The design hypothesis is that the insulinotropic effect of GLP-1 would restrain the hyperglycaemic action of glucagon.

As a result, six 12-mer peptides (termed PP01–PP06) were successfully selected (Fig. 1 and Table 1) and then fused to OXM (3–37) to produce PP07–PP12 (Table 1), which have enhanced GLP-1R activation potency. The *in vitro* results of binding affinity tests showed that PP11 showed balanced GLP-1R and GcgR activation potency. For this reason, this peptide was selected to make further fatty chain modifications in order to increase its plasma stability and develop long-acting fatty chain-modified OXM-based dual receptor agonist conjugates. As shown in Fig. 2, twelve fatty chain-modified OXM analogues (PP13–PP24) were designed and synthesized. Then, the dual receptor activation potency was accessed in stably expressed CHO cell line using native GLP-1, glucagon and OXM as controls. Results suggested that lysine-specific conjugations to the N- or C-terminal affect the receptor activation potency. We also found that the dual receptor activation potency was hardly independent of the fatty chain length as the selected analogues (PP16–PP18) showed similar receptor activation potency (Table 2). Hence, we selected PP18 for further *in vitro* and *in vivo* efficacy evaluation. Furthermore, the *in vitro* plasma stability test and multiple IPGTTs showed that PP18, modified with fatty acid chain (C18), showed better *in vitro* plasma stability and *in vivo* glucose-lowering durability compared to PP16–PP17 (Fig. 3 and 4).

In signaling studies using CHO cells stably expressing GLP-1R or GcgR, PP11 and PP18 potently stimulated cAMP accumulation through either receptor. The potencies were both similar to GLP-1 (Fig. 5A) and a little weaker than glucagon in these assays (Fig. 5B). We further utilized the cells expressing both receptors to assess the function of cAMP accumulation and the response to increased cAMP compared to either native single glucagon or GLP-1 (Fig. 5C). Wild-type and transgenic mice lacking either GLP-1R or GcgR were used to assess the effects of PP11 and PP18 on insulin secretion and glucose homeostasis. In islets isolated from all three genotypes, both PP11 and PP18 stimulated insulin secretion in a glucose-dependent manner, and the deficiency of GcgR induced a significant increase in the level of secreted insulin (Fig. 6A–C). The glucose-lowering effects of PP11 and PP18 were further assessed *in vivo* using the IPGTT method in WT and receptor-deficient mice. As shown in Fig. 6D and F, PP18 improved glucose tolerance in both WT and GcgR^{−/−} mice. Interestingly, GLP-1R deficiency did not induce persistent hyperglycemia compared to what was observed in the saline group (Fig. 6E). This is possibly because the potency for the glucagon receptor is weaker *in vivo*.

The hypoglycaemic duration of PP18 was evaluated in DIO mice. As a result, PP18 showed much longer hypoglycaemic durations compared to native liraglutide for both doses (10 or 30 nmol kg^{−1}) (Fig. 7A and B). We further evaluated the phar-

macokinetic characteristics of PP18 (30 nmol kg^{−1}, single i.v. injection) in SD rats using a liquid chromatography mass spectrometry (LC-MS) method to identify the long-acting hypoglycaemic duration. The maximum concentration was observed to be about 200 ng mL^{−1} at the first time point after dosing. The *in vivo* half-life of PP18 was approximately 37.5 h, which supports a twice-weekly dosing regimen (Fig. 7C).

Chronic treatment with both doses of PP18 enhanced the correction of excessive caloric intake, fat distribution, and poor glycaemic control in the insulin-resistant DIO mice. This was reflected in a significant decrease in food intake (Fig. 8A), body weight (Fig. 8C), insulin resistance (Fig. 8D), fat percentage (Fig. 8E), and HbA1c levels (Fig. 8F). Furthermore, there were improved abnormal blood biochemical indexes, such as TC, TG, and LDL (Fig. 8G). Notably, the administration of the co-agonist induced significant decreases in fat mass in DIO mice compared to liraglutide-treated mice. This emphasizes that glucagon significantly contributes to the metabolic effects, particularly to the body weight reducing effects of PP18 (Fig. 8E). In line with the capability of PP18 to improve insulin resistance, chronic treatment of this co-agonist significantly increased the number of Ki-67-positive cells (Fig. 9A, B, Fig. S3A†), and it markedly reduced the caspase-3 fraction (Fig. 9C and Fig. S3B†) in the pancreas of DIO mice. These are measures of islet-cell proliferation and apoptosis.

Experimental

Materials

The Ph.D.-12 phage library (New England Biolabs, Beverly, UK) was used to discover high-affinity GLP-1R agonists. All of the selected and side-chain modified peptides were obtained from Genscript Co., Ltd using standard Fmoc/*t*Bu solid-phase peptide synthesis protocols. An orthogonal protecting group strategy was employed to allow site-specific conjugation of the fatty acid moiety to lysine, following the synthesis of the linear sequence.

Identification of peptides

The purity of synthetic peptides was identified using reversed high-performance liquid chromatography (RP-HPLC, Agilent, USA) with a Inertsil ODS-SP C18 column (Shimadzu, 4.6 × 250 mm, 5 mm) and eluted with acetonitrile containing 0.1% trifluoroacetic acid (TFA) at a flow rate of 1 mL min^{−1} (detection wavelength, 214 nm). The mass of peptides was detected using matrix-assisted laser desorption/ionization time-of-flight mass spectrometry (MALDI-TOF/MS, Bruker, Germany) according to the user's manual.

Animals

Mice were group-housed in a temperature-controlled (at 22 ± 2 °C) environment with free access to food and water in a 12 h light : 12 h dark cycle. Male DIO mice and male SD rats were purchased from Joinn Laboratories, Inc. (Beijing, China). GLP-1R-null and GcgR-null mice were purchased from WuXi

AppTec Co., Ltd (Shanghai, China). The two strains of knock-out mice were backcrossed onto the C57BL/6 genetic background, and wild-type littermates were bred in-house and fed a standard chow diet. All studies were approved by and performed according to the guidelines of the Institutional Animal Care and Use Committee of the WuXi AppTec Co., Ltd and Joynn Laboratories, and the approval codes are ACU17-1112 and ACU18-179.

Discovery of novel GLP-1R agonists

The Ph.D.-12 phage library (New England Biolabs, USA) which contains random sequences of 12-mer peptide (library capacity, $\sim 10^9$) applied in the discovery of novel GLP-1R agonists was performed using phage display technology, as previously reported.^{26–29} In brief, the purified GLP-1R extracellular domain (ECD) (purity >98%) was dissolved in PBS (0.01 M, pH 7.0) and then coated on a 96-well plate. According to the phage library kit instruction, we conducted consecutive 4 rounds of screening with the GLP-1 ECD as the target to obtain the phage which express the peptides with high affinity for it. Following each round of selection, genes encoding the active peptides were recovered by PCR and subcloned to generate an enriched library used for the next round of selection. The selected phage was further propagated with *E. coli* (ER 2738 strain). The sequences of obtained peptides were accurately detected by using the 96 gIII (5'-CCCTCATAGTTAGCGTAACG-3'), a universal primer, for the DNA sequencing.

Surface plasmon resonance (SPR) measurements

SPR measurements were performed with a Biacore T200 system (GE Health, Boston, MA, America) for evaluating the binding affinity of selected peptides for GLP-1 and glucagon. In brief, the GLP-1R or GcgR ECD was immobilized using amine-coupling chemistry.³⁰ To collect binding parameters, different concentrations of peptides dissolved in buffer solution (36 mM $\text{Na}_2\text{HPO}_4 \cdot 7\text{H}_2\text{O}$, 70 mM NaCl, pH 7.4) were loaded at a flow velocity of approximately $10 \mu\text{L min}^{-1}$. The association and dissociation times of the complex were both set at ten minutes. The other experimental details were carried out according to the user's manual of Biacore T200.

Plasma stability test

PP11 and PP18 were incubated in rat plasma at 37 °C for 24 h. Plasma samples were aliquoted from the incubation solution at 0, 4, 8, 12, 16 and 24 h time points. Reaction products of OXM-based analogues were detected using liquid chromatography mass spectrometry (LC-MS) technology, and degradation is expressed as % of the initial intact peptide.

In vitro pharmacology of OXM analogues

CHO cells expressing either human GLP-1R or GcgR, or both were used to determine the potency of PP11 and PP18 to stimulate cAMP accumulation. Assays were performed as previously described,³¹ and cells were assayed for cAMP using homogeneous time-resolved fluorescence technology (Cisbio Bioassays, France). Pancreatic beta cells and human adipocytes

were obtained from ZenBio Inc., and they were used in accordance with established protocols.

Islet insulin secretion and glucose tolerance test

Islets were isolated from the pancreases of WT, GLP-1R^{-/-} and GcgR^{-/-} mice after the collagenase IV (Sigma, USA) digestion, and then hand-picked 5 times into fresh RPMI 1640 media (Thermo Fisher, USA) according to the previously reported method.^{32,33} For the genipin treatment of isolated islets, different treatments at 10 or 30 mM were incubated with isolated islets and maintained throughout.

Glucose tolerance tests were performed in wild-type and GLP-1R-null C57BL/6 mice. After an overnight fast, the mice were subcutaneously dosed with saline, OXM, liraglutide, or OXM-based analogues (30 nmol kg^{-1}). Then, they were challenged with an intraperitoneal bolus of 2 g kg^{-1} glucose half an hour later. Then, blood glucose and insulin levels were detected using glucometers (JNJ, USA) and insulin ELISA kits (Merck, Germany), respectively, pre-dose and at 15, 30, 45, 60, and 120 min post-dose. Area under the curve (AUC) calculations were obtained from the glucose concentrations measured between 0 and 120 minutes.

Hypoglycemic duration tests

Under non-fasting conditions, male type 2 diabetic rats received a single s.c. injection of PBS, liraglutide (10 nmol kg^{-1}) and PP18 (10 and 30 nmol kg^{-1}). Blood samples were subsequently collected from tail veins pre-dose and at 0.5, 1, 2, 4, 8, 16, 24, 48, 72, and 96 h. BGLs were detected using a glucometer (Bayer, Germany). Glucose-lowering durations under a BGL of 8.35 mmol L^{-1} were also checked.

Pharmacokinetics test

Two groups of six-week-old SD rats were administered a single subcutaneous dose of OXM or PP18 (30 nmol kg^{-1}). Then, blood was sampled pre-dose and at 0.5, 1, 2, 4, 8, 24, 48, 72, and 96 h post-dose. Plasma concentration levels of PP18 and OXM were detected using an established liquid chromatography-mass spectrometry (LC-MS) method and a human oxymodulin ELISA kit, respectively.

Chronic in vivo studies

The DIO mice were s.c. injected with saline, liraglutide (10 nmol kg^{-1}), or PP18 (10 or 30 nmol kg^{-1}) once daily for 4 weeks. Body weight, food intake, and water consumption were measured daily. DIO mice were subjected to an intraperitoneal glucose tolerance test (IPGTT) at weeks 0, 4, and 5 to evaluate the advancement of diabetes. HbA1c, triglycerides (TG), total cholesterol (TC), high-density lipoprotein (HDL), and low-density lipoprotein (LDL) levels were measured after the treatment using an AU680 automatic biochemical analyzer (Beckman Coulter, Germany). Fat mass composition was measured with nuclear magnetic resonance technology using an EFT-60/90 NMR spectrometer (Anasazi, America). The quantification of Ki-67 or caspase-3 was measured by islet-cell proliferation or apoptosis, respectively. The caspase-3 fraction,

the number of Ki-67-positive beta cells, and the total number of islets were measured as previously reported.³⁴

Data analysis

All measured variables are presented as mean \pm SD. Differences in all parameters were tested using one-way ANOVA. *P* values lower than 0.05 were considered significant.

Conclusions

In summary, the present study demonstrates that peptide fusion and fatty acid chain modification brought PP18 a balanced potency for GcgR/GLIP-1R *in vitro* and long-acting antidiabetic characteristics, respectively. Chronic treatment of PP18 in DIO mice significantly reduced food intake, reduced body weight, reduced the fat percentage, improved insulin resistance, improved abnormal blood biochemical indexes, and improved the function of islet beta cells. Overall, the pre-clinical data presented here demonstrate that PP18 is a potent dual agonist for GLP-1R and GcgR that activates both receptors *in vitro* and *in vivo*, and it offers better weight loss compared to selective GLP-1R agonist therapy in DIO mice. Thus, it may provide a novel therapeutic approach to treat T2DM and obesity.

Author contributions

Design and analysis of ideas, L. Z. and L. S.; methodology, B. W.; resources, L. W.; writing—original draft preparation, L. Z.; writing—review and editing, L. S.; methodology, experimental operation, X. Z.

Conflicts of interest

The authors declare no conflict of interest.

Acknowledgements

We thank Mogoedit for its linguistic assistance during the preparation of this manuscript.

Notes and references

- 1 A. Chaudhury, C. Duvoor, V. S. Reddy Dendi, S. Kraleti, A. Chada, R. Ravilla, A. Marco, N. S. Shekhawat, M. T. Montales, K. Kuriakose, A. Sasapu, A. Beebe, N. Patil, C. K. Musham, G. P. Lohani and W. Mirza, *Front. Endocrinol.*, 2017, **8**, 1–12.
- 2 A. American Diabetes, *Diabetes Care*, 2012, **35**(Suppl 1), S64–S71.
- 3 A. Kervran, P. Blache and D. Bataille, *Endocrinology*, 1987, **121**, 704–713.
- 4 L. Gros, B. Thorens, D. Bataille and A. Kervran, *Endocrinology*, 1993, **133**, 631–638.
- 5 M. A. Cohen, S. M. Ellis, C. W. Le Roux, R. L. Batterham, A. Park, M. Patterson, G. S. Frost, M. A. Ghatei and S. R. Bloom, *J. Clin. Endocrinol. Metab.*, 2003, **88**, 4696–4701.
- 6 K. Wynne, A. J. Park, C. J. Small, K. Meeran, M. A. Ghatei, G. S. Frost and S. R. Bloom, *Int. J. Obes.*, 2006, **30**, 1729–1736.
- 7 C. L. Dakin, C. J. Small, R. L. Batterham, N. M. Neary, M. A. Cohen, M. Patterson, M. A. Ghatei and S. R. Bloom, *Endocrinology*, 2004, **145**, 2687–2695.
- 8 L. L. Baggio, Q. Huang, T. J. Brown and D. J. Drucker, *Gastroenterology*, 2004, **127**, 546–558.
- 9 A. Maida, J. A. Lovshin, L. L. Baggio and D. J. Drucker, *Endocrinology*, 2008, **149**, 5670–5678.
- 10 A. Pocai, *Mol. Metab.*, 2014, **3**, 241–251.
- 11 M. R. Druce, J. S. Minnion, B. C. T. Field, S. R. Patel, J. C. Shillito, M. Tilby, K. E. L. Beale, K. G. Murphy, M. A. Ghatei and S. R. Bloom, *Endocrinology*, 2009, **150**, 1712–1721.
- 12 L. H. Zhao, Y. Yin, D. Yang, B. Liu, L. Hou, X. Wang, K. Pal, Y. Jiang, Y. Feng, X. Cai, A. Dai, M. Liu, M. W. Wang, K. Melcher and H. E. Xu, *J. Biol. Chem.*, 2016, **291**, 15119–15130.
- 13 A. Santoprete, E. Capito, P. E. Carrington, A. Pocai, M. Finotto, A. Langella, P. Ingallinella, K. Zytke, S. Bufali, S. Cianetti, M. Veneziano, F. Bonelli, L. Zhu, E. Monteagudo, D. J. Marsh, R. Sinharoy, E. Bianchi and A. Pessi, *J. Pept. Sci.*, 2011, **17**, 270–280.
- 14 V. K. Bhat, B. D. Kerr, P. R. Flatt and V. A. Gault, *Biochem. Pharmacol.*, 2013, **85**, 1655–1662.
- 15 B. D. Kerr, P. R. Flatt and V. A. Gault, *Biochem. Pharmacol.*, 2010, **80**, 1727–1735.
- 16 J. Lau, P. Bloch, L. Schaffer, I. Pettersson, J. Spetzler, J. Kofoed, K. Madsen, L. B. Knudsen, J. McGuire, D. B. Steensgaard, H. M. Strauss, D. X. Gram, S. M. Knudsen, F. S. Nielsen, P. Thygesen, S. Reedtz-Runge and T. Kruse, *J. Med. Chem.*, 2015, **58**, 7370–7380.
- 17 K. Madsen, L. B. Knudsen, H. Agersoe, P. F. Nielsen, H. Thogersen, M. Wilken and N. L. Johansen, *J. Med. Chem.*, 2007, **50**, 6126–6132.
- 18 D. B. Steensgaard, J. K. Thomsen, H. B. Olsen and L. B. Knudsen, *Diabetes*, 2008, **57**, A164.
- 19 J. Lau, P. Bloch, L. Schaffer, I. Pettersson, J. Spetzler, J. Kofoed, K. Madsen, L. B. Knudsen, J. McGuire, D. B. Steensgaard, H. M. Strauss, D. X. Gram, S. M. Knudsen, F. S. Nielsen, P. Thygesen, S. Reedtz-Runge and T. Kruse, *J. Med. Chem.*, 2015, **58**, 7370–7380.
- 20 A. Peters, *Am. J. Med.*, 2010, **123**, S28–S37.
- 21 D. J. Drucker, *Cell Metab.*, 2006, **3**, 153–165.
- 22 B. Finan, B. Yang, N. Ottaway, D. L. Smiley, T. Ma, C. Clemmensen, J. Chabenne, L. Zhang, K. M. Habegger, K. Fischer, J. E. Campbell, D. Sandoval, R. J. Seeley, K. Bleicher, S. Uhles, W. Riboulet, J. Funk, C. Hertel, S. Belli, E. Sebkova, K. Conde-Knape, A. Konkar, D. J. Drucker, V. Gelfanov, P. T. Pfluger, T. D. Muller,

- D. Perez-Tilve, R. D. DiMarchi and M. H. Tschop, *Nat. Med.*, 2015, **21**, 27–36.
- 23 V. K. Bhat, B. D. Kerr, S. Vasu, P. R. Flatt and V. A. Gault, *Diabetologia*, 2013, **56**, 1417–1424.
- 24 M. H. Tschop, B. Finan, C. Clemmensen, V. Gelfanov, D. Perez-Tilve, T. D. Muller and R. D. DiMarchi, *Cell Metab.*, 2016, **24**, 51–62.
- 25 J. W. Day, N. Ottaway, J. T. Patterson, V. Gelfanov, D. Smiley, J. Gidda, H. Findeisen, D. Bruemmer, D. J. Drucker, N. Chaudhary, J. Holland, J. Hembree, W. Abplanalp, E. Grant, J. Ruehl, H. Wilson, H. Kirchner, S. H. Lockie, S. Hofmann, S. C. Woods, R. Nogueiras, P. T. Pfluger, D. Perez-Tilve, R. DiMarchi and M. H. Tschop, *Nat. Chem. Biol.*, 2009, **5**, 749–757.
- 26 X. Zhong, Z. Chen, Q. Chen, W. Zhao and Z. Chen, *Molecules*, 2019, **24**(4), 779.
- 27 L. R. Goulart and P. d. S. Santos, *Vaccine Design*, Humana Press, New York, NY, 2016.
- 28 M. Popkov, I. Lussier, V. Medvedkine, P. O. Estève, V. Alakhov and R. Mandeville, *Eur. J. Biochem.*, 1998, **251**, 155–163.
- 29 S. S. Sidhu, H. B. Lowman, B. C. Cunningham and J. A. Wells, *Methods Enzymol.*, 2000, **328**, 333–363.
- 30 R. L. Rich and D. G. Myszkka, *J. Mol. Recognit.*, 2001, **14**, 223–228.
- 31 T. Coskun, K. W. Sloop, C. Loghin, J. Alsina-Fernandez, S. Urva, K. B. Bokvist, X. Cui, D. A. Briere, O. Cabrera, W. C. Roell, U. Kuchibhotla, J. S. Moyers, C. T. Benson, R. E. Gimeno, D. A. D'Alessio and A. Haupt, *Mol. Metab.*, 2018, **18**, 3–14.
- 32 N. Seshadri, M. E. Jonasson, K. L. Hunt, B. Xiang, S. Cooper, M. B. Wheeler, V. W. Dolinsky and C. A. Doucette, *Mol. Metab.*, 2017, **6**, 760–769.
- 33 C. A. Robson-Doucette, S. Sultan, E. M. Allister, J. D. Wikstrom, V. Koshkin, A. Bhattacharjee, K. J. Prentice, S. B. Sereda, O. S. Shirihai and M. B. Wheeler, *Diabetes*, 2011, **60**, 3307–3307.
- 34 L. S. Dalboge, D. L. C. Almholt, T. S. R. Neerup, N. Vrang, J. Jelsing and K. Fosgerau, *J. Pharmacol. Exp. Ther.*, 2014, **350**, 353–360.